Received: 29 July 2022 | Revised: 31 October 2022 | Accepted: 11 November 2022

DOI: 10.1002/mrm.29543

RESEARCH ARTICLE

Magnetic Resonance in Medicine

Soy lecithin: A beneficial substance for adjusting the ADC in aqueous solutions to the values of biological tissues

Victor Fritz[1] | **Petros Martirosian**[1] | **Jürgen Machann**[1,2,3] | **Daniela Thorwarth**[4] | **Fritz Schick**[1,5]

[1]Section on Experimental Radiology, Department of Diagnostic and Interventional Radiology, University of Tübingen, Tübingen, Germany

[2]Institute for Diabetes Research and Metabolic Diseases of the Helmholtz Centre Munich at the University of Tübingen, Tübingen, Germany

[3]German Center for Diabetes Research (DZD), Neuherberg, Germany

[4]Section for Biomedical Physics, Department of Radiation Oncology, University of Tübingen, Tübingen, Germany

[5]Cluster of Excellence iFIT (EXC 2180) "Image Guided and Functionally Instructed Tumor Therapies", University of Tübingen, Tübingen, Germany

Correspondence
Victor Fritz, Section on Experimental Radiology, Department of Diagnostic and Interventional Radiology, University of Tübingen, Hoppe-Seyler-Str. 3, 72076 Tübingen, Germany.
Email: victor.fritz@med.uni-tuebingen.de

Funding information
German Research Foundation (DFG), Grant/Award Numbers: SCHI 498/14-1, TH 1528/6-1(PAK 997/1)

Purpose: To test soy lecithin as a substance added to water for the construction of MRI phantoms with tissue-like diffusion coefficients. The performance of soy lecithin was assessed for the useable range of adjustable ADC values, the degree of non-Gaussian diffusion, simultaneous effects on relaxation times, and spectral signal properties.

Methods: Aqueous soy lecithin solutions of different concentrations (0%, 0.5%, 1%, 2%, 3% …, 10%) and soy lecithin–agar gels were prepared and examined on a 3 Tesla clinical scanner at 18.5° ± 0.5°C. Echoplanar sequences (*b* values: 0–1000/3000 s/mm^2) were applied for ADC measurements. Quantitative relaxometry and MRS were performed for assessment of T_1, T_2, and detectable spectral components.

Results: The presence of soy lecithin significantly restricts the diffusion of water molecules and mimics the nearly Gaussian nature of diffusion observed in tissue (for *b* values <1000 s/mm^2). ADC values ranged from 2.02×10^{-3} mm^2/s to 0.48×10^{-3} mm^2/s and cover the entire physiological range reported on biological tissue. Measured T_1/T_2 values of pure lecithin solutions varied from 2685/2013 to 668/133 ms with increasing concentration. No characteristic signals of soy lecithin were observed in the MR spectrum. The addition of agar to the soy lecithin solutions allowed T_2 values to be well adjusted to typical values found in parenchymal tissue without affecting the soy lecithin–controlled ADC value.

Conclusion: Soy lecithin is a promising substance for the construction of diffusion phantoms with tissue-like ADC values. It provides several advantages over previously proposed substances, in particular a wide range of adjustable ADC values, the lack of additional ^{1}H-signals, and the possibility to adjust ADC and T_2 values (by adding agar) almost independently of each other.

KEYWORDS
ADC, diffusion phantom, DWI, relaxometry, soy lecithin

1 | INTRODUCTION

The ADC of water molecules as determined by DWI plays a crucial role in the diagnosis and assessment of a variety of tissue disorders, including cerebral infarctions, malignant lesions, and tissue fibrosis.[1–3] In oncology, the ADC is considered a promising biomarker for monitoring treatment response. It has been shown that the ADC value increases with a decrease of tumor cell density caused by the application of radiation therapy.[4–10] For a reliable use of ADC values as biomarkers, it is essential that measurements of ADC values of tissues are accurate and as consistent as possible.

Because accuracy and precision of measured ADC values are difficult to verify in patients, the construction of phantoms containing materials with known reference values is of great value to check the performance of imaging techniques and MRI systems. At best, ADC values of test materials can be adjusted flexibly and cover the entire range of values found in biological tissue (~2–0.5 [10^{-3} mm^2/s]). In addition to a wide range of adjustable ADC values, DWI phantoms should mimic other intrinsic tissue properties, such as T_2 relaxation times, but also limited diffusion kurtosis, as these properties have been shown to significantly affect the quantification of ADC values in biological tissue.[11,12] Although not explicitly stated as problematic in the literature, it is desirable that T_1 relaxation times of the DWI tissue-mimicking phantoms also reflect in vivo conditions.

Several DWI phantoms simulating predefined ADC values have already been presented.[13–17] They are mainly based on sucrose, polyethylene glycol, or polyvinylpyrrolidone, with the ADC value being controlled by the concentration of the solute or the measurement temperature. However, as already discussed in the literature,[15,17] all these substances bring with them different problems and disadvantages, such as a limited range of ADC values, strong reduction in T_2 relaxation time, and/or additional MR signal components with multiple spectral peaks. In addition, a relatively large amount of the respective substance is often required to significantly reduce the ADC of the solvent.

For this reason, we searched for a substance that solves the aforementioned problems with the materials proposed thus far for diffusion phantoms: in short, the ADC-modifying substance should essentially fulfill 4 criteria: (1) coverage of the full range of ADC values found in biological tissue, (2) mimicking the approximate Gaussian nature of water diffusion in tissue for b values <1000 s/mm^2, (3) a relatively small effect on the T_2 relaxation time so that the ADC and T_2 values can be adjusted independently by adding a T_2 modifier, and (4) a ^1H spectrum without undesired lines from the added substance because interfering signals can lead to artifacts and inaccuracies in quantitative measurements. As mentioned above, it is also desirable that the T_1 relaxation times are within the range of values found in biological tissue.

Recently, soy lecithin, a naturally occurring emulsifier that is mainly used in the food industry, has been identified as an attractive agent for the preparation of tissue-like MRI fat–water phantoms.[18,19] In former experiments, it was found that dissolving small quantities of soy lecithin in aqueous solution does not lead to visible signals in spectra with a relatively short TE of 10 ms.[18]

Soy lecithin molecules are a class of phospholipids that, due to their amphiphilic nature, form self-assembled aggregates, so-called micelles, in aqueous solution. Depending on the concentration, temperature, and ionic environment, different shapes of aggregates such as bilayers or liposomes can form (Figure 1).[20,21] These molecular constructs are well suited to act as barriers and impede diffusion of water protons, analogous to cellular structures in biological tissues. With this background, soy lecithin seems to be a promising inexpensive (20–30 euros per 250 grams) substance for use in diffusion MRI phantoms that might meet the criteria mentioned above.

The aim of this work was to systematically investigate the MR-related properties of aqueous solutions with soy lecithin. The effects on the ADC and on the relaxation times (T_1 and T_2) of water were systematically investigated using different concentrations (0%–10%) of soy lecithin. The grade of non-Gaussian diffusion was determined using diffusion kurtosis imaging. To see if soy lecithin remains "MR invisible" at higher concentrations or leads to detectable additional spectral signals at proton resonance frequencies, the highest concentrated solution (10%) was also examined by ^1H MRS. In addition, signals of a 10% soy lecithin solution in deuterium oxide (D_2O) and pure D_2O were recorded and compared using a gradient echo sequence with short TE in order to exclude possible signal contributions from soy lecithin at the water resonance frequency. Series of measurements tested whether T_2 of the aqueous soy lecithin solutions can be controlled independently of the ADC value by adding agar as a T_2 modifier.

2 | METHODS

2.1 | Sample preparation and measurement setup

Twelve tubes with aqueous solutions of soy lecithin (Carl Roth, Karlsruhe, Germany) were prepared in volumes of 50 mL. The concentration of dissolved soy lecithin varied from 0% to a maximum of 10% (0%, 0.5%, 1%, 2%, 3% …,

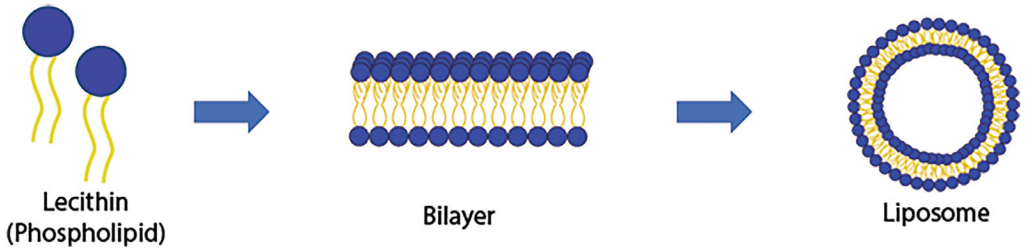

FIGURE 1 Schematic representation of micellization of lecithin molecules in aqueous solution. Depending on concentration, temperature, and ionic environment, different types of aggregates form (e.g., bilayer, liposomes)[20,21]

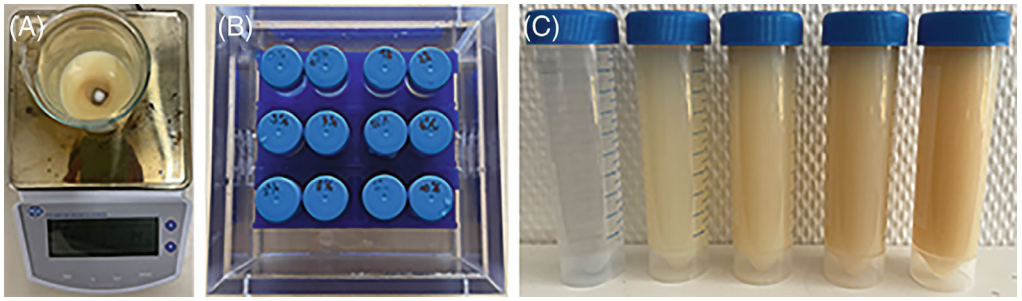

FIGURE 2 Sample photos of (A) the preparation process of the aqueous soy lecithin solutions. The solutions were prepared by dissolving soy lecithin in distilled water using a 125 mL glass beaker and magnetic stirring. (B) The MRI phantom with 12 CELLSTAR tubes (Greiner Bio-One, Frickenhausen, Germany) containing aqueous soy lecithin solutions of different concentrations. The surroundings of the tubes were filled with water to reduce susceptibility effects at the wall of the tubes. (C) Soy lecithin solutions with different concentrations (from left to right: 0%, 2%, 4%, 6%, 8%)

10%) with respect to the solvent. The solutions were prepared by dissolving soy lecithin in distilled water using a 125 mL glass beaker and magnetic stirring (PCE-MSR 300, PCE Instruments, Meschede, Germany) at 650 revolutions per minute for 20 min at room temperature (Figure 2A). All samples were prepared under the same conditions.

Furthermore, a series of soy lecithin–agar gels was prepared to investigate whether T_2 of the aqueous soy lecithin solutions can be controlled independently of the ADC value by the addition of agar. The effects of adding agar on ADC and T_1 values of the aqueous soy lecithin solutions were also monitored. For this purpose, the concentration of agar was varied (1%, 2%, 3%, 4%), whereas the concentration of soy lecithin was kept constant. Series of measurements were performed for 3 different fixed concentrations of soy lecithin of 2%, 4%, and 6%. Because agar requires high temperature to be solved, the soy lecithin and agar portions were first dissolved separately and then mixed. The aqueous soy lecithin solutions were prepared as described above. The agar solution was prepared by completely dissolving the appropriate amount of agar (Agar powdered, AppliChem Panreac, Darmstadt, Germany) in distilled water using a microwave heater. The agar solution was then cooled, and once the temperature of the solution dropped below 70°C, the aqueous soy lecithin solution was added with gentle stirring to obtain a homogeneous mixture.

After preparation, all samples were stored in sterilized CELLSTAR polypropylene tubes (Greiner Bio-One, Frickenhausen, Germany) and fixed in a square MRI phantom for measurement (Figure 2B,C). The surroundings of the tubes were filled with water in order to reduce susceptibility effects at the wall of the tubes.

To avoid temperature bias, all samples were stored overnight in the scanner room prior to measurements to ensure all samples were at the same measurement temperature. The temperature was measured with an alcohol thermometer in the water around the tubes before each measurement (18.5 ± 0.5°C).

2.2 | Data acquisition and analysis

Imaging and spectroscopy were performed on a clinical, whole-body 3.0 Tesla MR system (Magnetom Prisma^{fit}, Siemens Healthcare, Erlangen, Germany) using an 18-channel body array coil. All measurements were performed 3 times, and all data were processed offline using in-house developed software (MatLab R2020b, MathWorks, Natick, MA).

DWI was performed using a readout-segmented spin-echo EPI sequence with a pair of monopolar diffusion sensitizing gradients and 4 different b values (0, 50, 500, 1000 s/mm^2). TR and TE were set to 5000 and 48 ms, respectively. Other parameters include FOV = 200 × 200 mm, matrix size = 128 × 128, slice thickness = 5 mm, number of slices = 10, slice in coronal plane, bandwidth = 751 Hz/px, GRAPPA factor = 2, fat suppression = fat sat. standard, number of readout segments = 7, δ = 6.9 ms, and Δ = 21.7 ms. Noise-corrected ADC maps were calculated from the acquisitions with multiple b values using a log-linear fitting of the signal intensities: $\ln(S/S_0) = -ADC \cdot b + c$.

Diffusion kurtosis imaging was performed using the same DWI sequence type as described above. In contrast to the former measurements, 8 b values 0, 50, 500, 1000, 1500, 2000, 2500, 3000 s/mm^2 were chosen, and the following modified parameters were applied: TE = 56 ms, δ = 10.9 ms, and Δ = 25.7 ms. The natural logarithm of the signal intensities (S/S_0) was plotted as a function of b value and compared with a linear signal decay observed with free or Gaussian diffusion in pure liquids. The mean kurtosis value K was calculated in each solution by pixel-wise fitting the signal intensities as a function of b value using the following diffusion kurtosis model: $\ln(S/S_0) = -\text{ADC} \cdot b + b^2 \cdot \text{ADC}^2 \cdot K/6 + c$. All 8 b values were used for the fitting procedure.

Measurements of T_1 were performed using a turbo spin-echo-based inversion-recovery pulse sequence with 9 different logarithmically equally spaced TIs (25–6400 ms). TR and TE were set to 10,000 ms and 9.9 ms, respectively. One slice was recorded in the coronal plane, which was positioned at the center of the samples. T_1 maps were calculated using a 3-parameter model for pixelwise mono-exponential fitting of the measured signal intensities: $S = S_0 \cdot [1 - a \cdot \exp(-T_I/T_1) + \exp(-TR/T_1)]$.

Relaxation times T_2 were assessed in the same slice using a Carr-Purcell-Meiboom-Gill spin-echo pulse sequence with a TR of 6000 ms and 32 TE values ranging from 50 ms to 1600 ms (increment 50 ms). Because the addition of agar leads to a strong reduction in the T_2 values, the measurement for the soy lecithin–agar gels was carried out with shorter TEs in the range of 10–320 ms (incr. 10 ms). T_2 maps were calculated by pixel-wise monoexponential fitting of the measured signal intensities using a 3-parameter model: $S = S_0 \cdot \exp(-TE/T_2) + c$. All signal values were noise-corrected before being used for the fit procedure in the specified model.

ADC, T_1, and T_2 values of each sample were determined from circular regions of interest in the calculated parametric maps. The mean and SD were determined from all measurements.

Single voxel STEAM spectra were recorded with short TE from the highest concentrated soy lecithin solution (10% in water) to check whether signals from ^{1}H atoms in soy lecithin appear in the spectra, which could lead to unwanted interference in MRI experiments. Parameters for measuring a cubic volume of interest (10 × 10 × 10 mm) positioned in the center of the sample were TR 5000 ms, TE = 20 ms, bandwidth 1200 Hz, 16 acquisitions. In order to investigate possible signal contributions from soy lecithin at the water resonance frequency, signals of a 10% soy lecithin solution in D_2O and pure D_2O were recorded and compared using a gradient echo sequence with TE = 3 ms.

3 | RESULTS

DW images (b = 0 s/mm^2, b = 1000 s/mm^2), ADC, and relaxation time maps of the vials filled with aqueous soy lecithin solutions of different concentrations are shown in Figure 3A–3E. The vials were arranged as shown in Figure 3F. The parametric maps reveal a clear dependence of the ADC value and relaxation times on the concentration of dissolved soy lecithin in water. Chemical shift artifacts could not be observed in either the ADC or the T_1 and T_2 maps.

Table 1 summarizes the mean ADC, T_1, and T_2 values as a function of the concentration of dissolved soy lecithin. Both the ADC value and relaxation times show a decrease with increasing concentration of soy lecithin.

Even small amounts of soy lecithin considerably restrict the diffusion of the water protons (reduction of 20% at a concentration of 0.5%). The determined ADC values ranged from 2.02×10^{-3} mm^2/s for pure water to 0.48×10^{-3} mm^2/s for the sample with the highest concentration of dissolved soy lecithin (10%). It is striking that the ADC value and the concentration of soy lecithin show a nonlinear relationship. The change in ADC value as a function of soy lecithin concentration slightly decreases at higher concentrations (Figure 4).

Figure 5A shows the signal decay as a function of b value for a 5% soy lecithin solution. The dashed–dotted line represents a linear signal decay, which is expected for free or Gaussian water proton diffusion observed in pure liquids without barriers. It is obvious that the signal decay originating from the aqueous soy lecithin solutions at high b values deviates significantly from the expected values of Gaussian diffusion, indicating non-Gaussian diffusion in the aqueous soy lecithin solution. An increase of soy lecithin concentration was associated with an increase in the mean kurtosis value K (Figure 5B). Values ranged from 0 for pure water to ~0.5 for the highest concentrated soy lecithin solution.

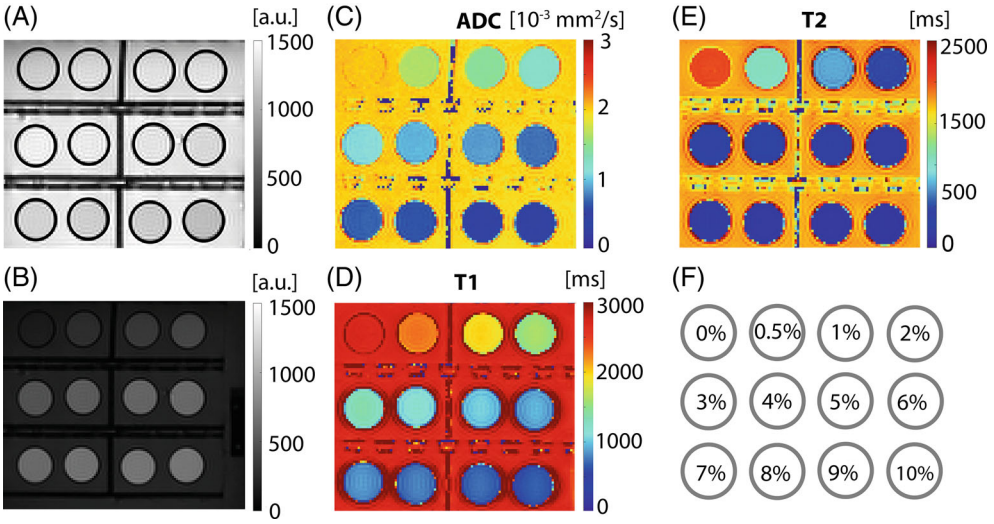

FIGURE 3 Images and parametric maps of the aqueous soy lecithin solutions of different concentrations in an MRI phantom. (A) DW image with $b = 0$ s/mm^2. (B) DW image with b = 1000 s/mm^2. (C) Parametric map of ADC values. (D) Parametric map of T_1 values. (E) Parametric map of T_2 values. (F) Illustration of the positions of the aqueous soy lecithin solutions with different concentrations in the phantom

TABLE 1 ADC, T_1, and T_2 values of aqueous soy lecithin solutions as a function of soy lecithin concentration.

Concentration (%)	ADC (10^{-3} mm^2/s)	T_1 (ms)	T_2 (ms)
0	2.02 ± 0.02	2685 ± 67	2013 ± 41
0.5	1.59 ± 0.02	2286 ± 70	1089 ± 28
1	1.42 ± 0.02	1993 ± 65	792 ± 37
2	1.22 ± 0.01	1618 ± 48	506 ± 34
3	1.08 ± 0.01	1359 ± 35	375 ± 23
4	0.94 ± 0.01	1170 ± 23	293 ± 9
5	0.86 ± 0.01	1030 ± 18	242 ± 6
6	0.73 ± 0.02	929 ± 13	207 ± 5
7	0.68 ± 0.02	843 ± 8	183 ± 3
8	0.61 ± 0.02	778 ± 6	164 ± 2
9	0.52 ± 0.03	717 ± 4	148 ± 1
10	0.48 ± 0.02	668 ± 4	133 ± 2

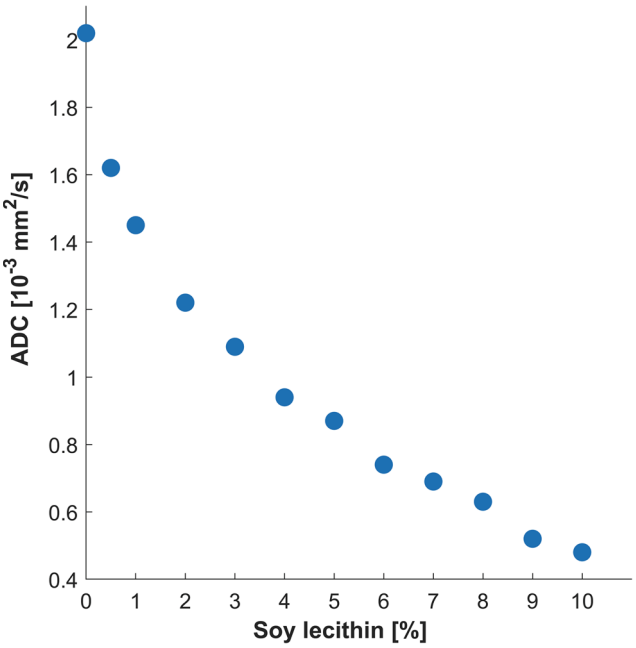

FIGURE 4 ADC values of the aqueous soy lecithin solutions as a function of the soy lecithin concentration.

As mentioned above, changing the soy lecithin concentration not only influenced the ADC value but also the relaxation times of the aqueous solutions. Measured T_1/T_2 values ranged from 2685 ms/2013 ms for pure water to 668 ms/133 ms for the highest concentration of soy lecithin.

Figure 6 shows a representative ^{1}H spectrum obtained from a highly concentrated (10%) aqueous soy lecithin solution, which was acquired to check for potential soy lecithin signals at higher concentrations. However, apart from the water signal at 4.75 ppm, no distinct signals could be detected in the STEAM spectrum recoded with TE = 20 ms. Only when zooming in closer, a small signal shoulder is guessed near the water signal, which, however, seems to be close to the noise level (red arrow in Figure 6).

This result agrees well with the fact that no chemical shift artifacts were observed in the ADC and relaxation time maps. Signal intensities recorded by gradient echo imaging from solutions of 10% soy lecithin dissolved in D_2O confirmed the absence of direct signal contributions from soy lecithin, as signal intensities were not increased compared to results from pure D_2O (99.9%).

Figure 7A–7C shows ADC and relaxation time maps of the soy lecithin–agar gels. Vials were arranged in the order of increasing agar concentrations (from left to right), whereas soy lecithin concentration increases from top to bottom (Figure 7D). The numbers in the parentheses indicate the soy lecithin or agar concentrations (soy

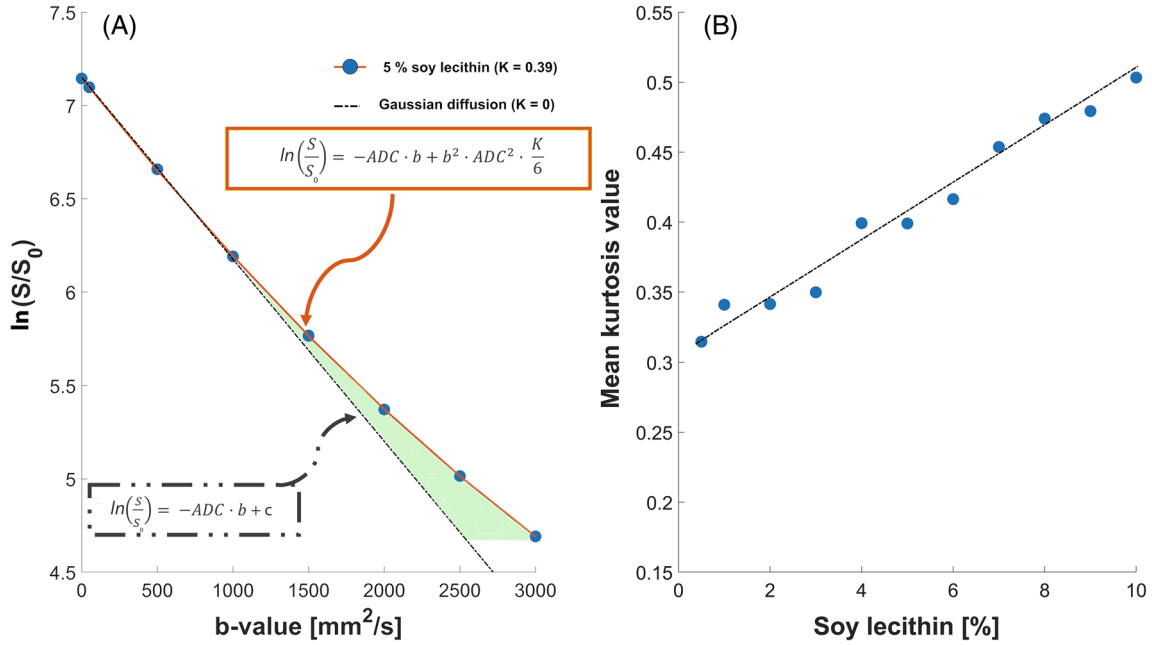

FIGURE 5 (A) Signal decay as a function of *b* value for a 5% soy lecithin solution. The dashed–dotted line represents the linear signal decay for free or Gaussian water proton diffusion observed in pure liquids without barriers. (B) Mean kurtosis value *K* of the aqueous soy lecithin solutions as a function of the soy lecithin concentration

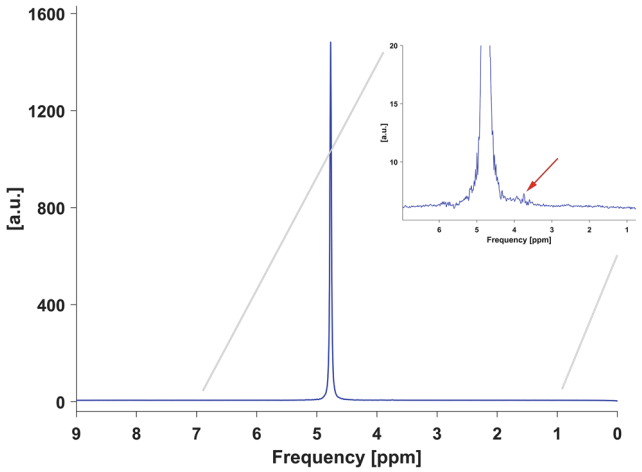

FIGURE 6 ^{1}H spectrum obtained from a highly concentrated (10%) aqueous soy lecithin solution using single voxel STEAM spectroscopy with TE = 20 ms. Apart from the water signal at 4.75 ppm, no distinct signals could be detected. When zooming in closer, a small signal shoulder is guessed near the water signal, which, however, seems to be close to the noise level (red arrow)

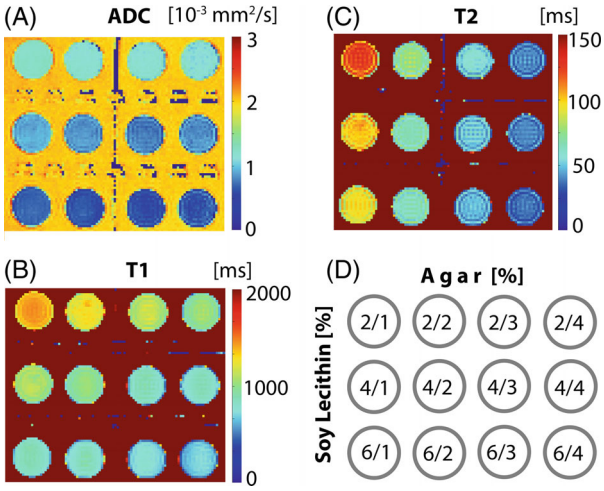

FIGURE 7 (A) Parametric map of measured ADC values as a function of agar or soy lecithin concentration. (B) Parametric map of measured T_1 values as a function of agar or soy lecithin concentration. (C) Parametric map of measured T_2 values as a function of agar or soy lecithin concentration. (D) Illustration of the positions of the soy lecithin–agar gels in the phantom. Vials were arranged in the order in which agar concentration increases from left to right and soy lecithin concentration increases from top to bottom. The numbers in the parentheses indicate the soy lecithin or agar concentration (soy lecithin/agar)

lecithin/agar). Table 2 summarizes the mean ADC, T_1, and T_2 values of the gels as a function of agar and soy lecithin concentration, respectively. The addition of agar to the aqueous soy lecithin solutions resulted in a strong decrease of the T_2 relaxation time (Figure 7C). The T_2 values of the aqueous soy lecithin solutions were reduced to a value of 38 ms by adding 4% of agar. On the other hand, the ADC value of the aqueous soy lecithin solutions was hardly affected with increasing agar concentration (Figure 7A). Comparing the T_2 and ADC values of the gels leads to the

TABLE 2 ADC, T_1, and T_2 values of the soy lecithin–agar gels as a function of agar or soy lecithin concentration.

Soy lecithin (%)	Agar (%)			
	1	2	3	4
2				
ADC (10^{-3} mm^2/s)	1.24 ± 0.02	1.18 ± 0.03	1.17 ± 0.03	1.12 ± 0.04
T_1 (ms)	1456 ± 13	1283 ± 18	1165 ± 24	1057 ± 26
T_2 (ms)	125 ± 5	78 ± 4	57 ± 3	41 ± 4
4				
ADC (10^{-3} mm^2/s)	0.92 ± 0.03	0.85 ± 0.03	0.77 ± 0.04	0.83 ± 0.04
T_1 (ms)	1126 ± 18	1031 ± 10	881 ± 25	875 ± 14
T_2 (ms)	102 ± 3	66 ± 2	53 ± 5	41 ± 2
6				
ADC (10^{-3} mm^2/s)	0.71 ± 0.02	0.66 ± 0.04	0.59 ± 0.04	0.63 ± 0.05
T_1 (ms)	884 ± 14	877 ± 23	770 ± 23	718 ± 16
T_2 (ms)	96 ± 3	64 ± 4	49 ± 2	38 ± 2

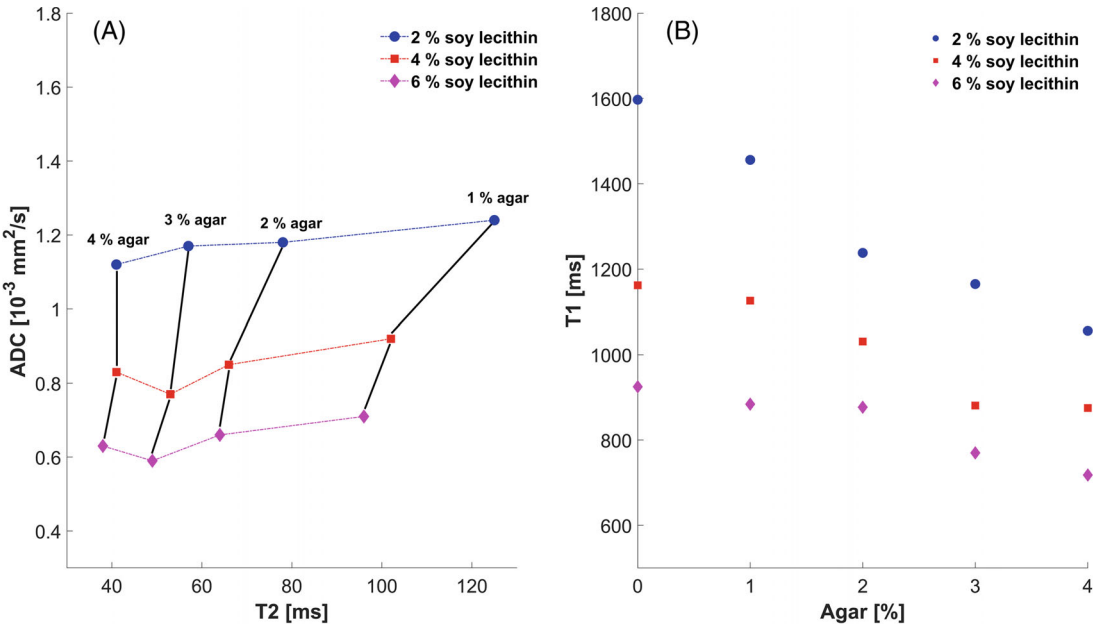

FIGURE 8 (A) Variation of the ADC and T_2 values of the soy lecithin–agar gels depending on the agar and soy lecithin concentration. (B) T_1 values of the aqueous soy lecithin solutions are given as a function of agar concentration

conclusion that the T_2 value is mainly dependent on the amount of agar, whereas the ADC is mainly determined by the amount of soy lecithin (Figure 8A). With increasing concentration of agar, the influence of soy lecithin on T_2 becomes more and more negligible. In addition to reducing T_2, agar caused a slight decrease in T_1 of the gels with increasing concentration. On the other hand, the influence of agar on T_1 decreased with lecithin concentration (Figure 8B) (Table 2).

4 | DISCUSSION

Soy lecithin is a relatively cheap natural emulsifier that provides stable emulsions for MR experiments.[18] Because soy lecithin was found to significantly alter the ADC of water in aqueous solutions, the potential of soy lecithin to generate DWI phantoms with predefined tissue-like ADC values was evaluated in this work. To this end, series of systematic measurements were performed on aqueous soy

lecithin solutions and soy lecithin agar gels, investigating the influences on diffusion, relaxation times, and the signal components that occur.

With increasing concentration of soy lecithin in aqueous solution, the ADC value of water steadily decreased. The ADC values achieved were between 2.02×10^{-3} mm^2/s and 0.48×10^{-3} mm^2/s and thus cover a large range of values that includes the ADCs of most biological tissues and malignant lesions (e.g., liver, prostate, spleen, pancreas, gray and white matter).[22–24] However, it was found that the ADC decrease was not linear with soy lecithin concentration, which was also observed for polyethylene glycol.[15]

To the authors' knowledge, no substance has yet been described in the literature that influences the ADC value of water to a comparable extent as soy lecithin. Previously proposed substances such as sucrose, polyvinylpyrrolidone, or polyethylene glycol require 5 to 10 times the concentration to simulate the same range of ADC values. As reported in Wang et al.,[17] 40% sucrose is required to achieve an ADC value of 0.61×10^{-3} mm^2/s, whereas only about 8% soy lecithin is required here. Soy lecithin thus enables flexible adjustment of the ADC value of water with low resource consumption. Diffusion kurtosis measurements revealed that the water diffusion within aqueous soy lecithin solutions (slightly) deviates from the Gaussian behavior ($K > 0$) at high b values. This could be explained by the concentration dependent micellization of soy lecithin molecules. In aqueous solutions, amphiphilic substances such as soy lecithin form self-assembled aggregates that act as barriers and thus restrict the self-diffusion of water protons, similar to intrinsic microstructures (e.g., cell membranes) in biological tissues. As the concentration of soy lecithin increased, the number and possibly the geometry/size of aggregates changed, and with it the associated restriction of water proton diffusion. The mean kurtosis value ranged from 0 for pure water to ~0.5 for the solution with the highest concentration (10%). In the latter case, kurtosis was in the same order of magnitude as reported from biological tissue.[25,26] This finding suggests that soy lecithin in aqueous solution is a promising substance that could mimic not only ADC values but also—in contrast to sucrose—the restricted diffusion of water in biological tissues. However, the mechanism by which the aqueous soy lecithin solutions generates restricted diffusion appears to be clearly different from that of biological tissue (or tumors). In particular, the concentration-dependent micelle morphology (in terms of size and geometry) is considered critical, as diffusion changes in tumors are understood to be due to changes in cell density without changes in basic cell geometry. In addition, the micelles formed are usually mobile and few 100 nm in size,[27] whereas the cell membranes in the tissues are immobile and their size is in the order of several micrometers. Therefore, further work is needed to study micelle formation in more detail and to understand how well they actually can mimic tissue microstructure. It needs to be investigated whether and to what extent the morphology (size/geometry) of the micelles changes as a function of the soy lecithin concentration but also of the temperature. Furthermore, relative intra-liposome/extra-liposome water volumes might be a source of non-Gaussian diffusion. It is also not yet examined how the kurtosis effects in soy lecithin solution change using higher b values and longer diffusion-sensitive time between dephasing and rephasing diffusion gradients (e.g., using stimulated echo sequences). In this context, another approach to mimic diffusion characteristics of tumor tissue should be mentioned, which was proposed by McHugh et al.[28] This group developed a biomimetic tumor tissue phantom using hollow polymer spheres with predefined sizes to mimic cells in tissues.

Like other ADC-modifying substances, soy lecithin causes a reduction in T_1 and T_2. The measurements indicated that the T_1 values of the aqueous solutions of soy lecithin were in the range of values that most biological tissues also exhibit (600–1800 ms).[29] Only solutions with low soy lecithin concentration (< 2%) presented T_1 values slightly above 1800 ms. However, these could be safely adjusted by adding T_1-active substances (e.g., gadolinium-diethylenetriamine pentaacetic acid or nickel chloride) to the soy lecithin solutions, but this was not pursued further in our experiments. Published studies have shown that the T_1 and T_2 values of aqueous solutions can be adjusted quite well independently by adding nickel chloride and agar as T_1 and T_2 modifiers, respectively.[30,31] However, possible interactions between nickel chloride and soy lecithin must then also be taken into account and investigated, which was not done in our study.

The T_2 values of the aqueous soy lecithin solutions ranged from 2013 to 133 ms, still well above the T_2 of almost all parenchymal tissues.[29] This seems to be another advantage of soy lecithin, as it offers the possibility to adjust the apparent diffusion coefficient and the T_2 relaxation time largely independently. As shown in this work, the ADC value can be controlled by the concentration of soy lecithin, whereas the T_2 values can be adjusted to the desired values by adding agar. The addition of agar to the aqueous soy lecithin solutions resulted in a large decrease in T_2 with no significant effect on ADC values and little effect on T_1. A similar approach was previously proposed by Gatidis et al.[15] This group used a mixture of polyethylene glycol (as ADC modifier) and gadobutrol (as T_2 modifier) to adjust ADC and T_2 values independently.

Another remarkable result of the present study is that soy lecithin, even at the highest concentration, did not

contribute any direct ^{1}H signal to the spectrum recorded at a (relatively) short TE of 20 ms. The lack of direct signals from soy lecithin was confirmed by gradient echo imaging of 10% soy lecithin dissolved in D_2O, where the signal intensity was equal to that of pure D_2O. One explanation could be that soy lecithin molecules, similar to phospholipids in the cell membranes of intact animal cells, have very limited mobility within the formed micelles, which in turn leads to an extremely short relaxation time ($T_2 < 1$ ms), making them undetectable in MRS or MRI measurements with TEs of a few milliseconds. This is particularly advantageous as solute signals could have undesirable effects and cause inaccuracies or even systematic errors in quantitative ADC measurements. For example, polyethylene glycol, which has a dominant signal at about 3.7 ppm, caused problems and distortions in the determination of the ADC value in polyethylene glycol-based DWI phantoms.[15]

However, there are also some potential limitations that should be mentioned. First, soy lecithin is a nature product; thus, unlike synthetic substances, the composition of soy lecithin may vary slightly in different product batches. This could make reproducibility difficult if different sources of soy lecithin are used. Second, because soy lecithin is an organic substance and the aqueous solutions may mold or rot after some time, a suitable fungicide and bactericide must probably be added to ensure the long-term stability of the phantoms. Third, the temperature dependence of the DW-MRI–derived parameters (ADC value, mean kurtosis) was not investigated. However, knowledge of temperature dependence is very important, especially when the phantom is used in multicenter studies in which temperature varies from site to site and over time. Therefore, temperature calibration curves as described by Wagner et al.[32] for polyvinylpyrrolidone phantoms are needed to make the application of soy lecithin–based diffusion phantoms practical. Furthermore, there might be a hysteresis effect due to a dependence of micelle composition on the temperature curve during phantom production, which has to be considered and further explored.

In summary, the systematic measurements carried out show that aqueous solutions of soy lecithin are a promising material for the construction of MRI diffusion phantoms with tissue-like diffusion coefficients. The use of soy lecithin fulfills the criteria mentioned at the beginning very well and offers several advantages over the substances used thus far. In addition, soy lecithin is nonhazardous, inexpensive, and easy to handle. However, there are still some problems regarding the influence of the manufacturing process and the durability but also the behavior when applying different DWI methods, which must be worked on and solved before using soy lecithin as a material for quantitative diffusion phantoms.

ACKNOWLEDGMENT

This work was supported and funded by the German Research Foundation (DFG) under grants SCHI 498/14-1, TH 1528/6-1 (package no. 997/1). Open Access funding enabled and organized by Projekt DEAL.

ORCID

Victor Fritz https://orcid.org/0000-0003-0601-9901
Jürgen Machann https://orcid.org/0000-0002-4458-5886

REFERENCES

1. Fung SH, Roccatagliata L, Gonzalez RG, Schaefer PW. MR diffusion imaging in ischemic stroke. *Neuroimaging Clin N Am*. 2011;21:345-377. xi, 377.
2. Malayeri AA, El Khouli RH, Zaheer A, et al. Principles and applications of diffusion-weighted imaging in cancer detection, staging, and treatment follow-up. *Radiographics*. 2011;31:1773-1791.
3. Taouli B, Chouli M, Martin AJ, Qayyum A, Coakley FV, Vilgrain V. Chronic hepatitis: role of diffusion-weighted imaging and diffusion tensor imaging for the diagnosis of liver fibrosis and inflammation. *J Magn Reson Imaging*. 2008;28:89-95.
4. Padhani AR, Liu G, Koh DM, et al. Diffusion-weighted magnetic resonance imaging as a cancer biomarker: consensus and recommendations. *Neoplasia*. 2009;11:102-125.
5. Park SY, Kim CK, Park BK, et al. Early changes in apparent diffusion coefficient from diffusion-weighted MR imaging during radiotherapy for prostate cancer. *Int J Radiat Oncol Biol Phys*. 2012;83:749-755.
6. Yang Y, Cao M, Sheng K, et al. Longitudinal diffusion MRI for treatment response assessment: preliminary experience using an MRI-guided tri-cobalt 60 radiotherapy system. *Med Phys*. 2016;43:1369-1373.
7. Mahmood F, Johannesen HH, Geertsen P, Hansen RH. Repeated diffusion MRI reveals earliest time point for stratification of radiotherapy response in brain metastases. *Phys Med Biol*. 2017;62:2990-3002.
8. van Houdt PJ, Yang Y, van der Heide UA. Quantitative magnetic resonance imaging for biological image-guided adaptive radiotherapy. *Front Oncol*. 2020;10:615643.
9. Patterson DM, Padhani AR, Collins DJ. Technology insight: water diffusion MRI—a potential new biomarker of response to cancer therapy. *Nat Clin Pract Oncol*. 2008;5:220-233.
10. Leibfarth S, Winter RM, Lyng H, Zips D, Thorwarth D. Potentials and challenges of diffusion-weighted magnetic resonance imaging in radiotherapy. *Clin Transl Radiat Oncol*. 2018;13:29-37.
11. Colagrande S, Belli G, Politi LS, Mannelli L, Pasquinelli F, Villari N. The influence of diffusion- and relaxation-related factors on signal intensity: an introductive guide to magnetic resonance diffusion-weighted imaging studies. *J Comput Assist Tomogr*. 2008;32:463-474.
12. Baltzer P, Mann RM, Iima M, et al. Diffusion-weighted imaging of the breast-a consensus and mission statement from the

EUSOBI international breast diffusion-weighted imaging working group. *Eur Radiol*. 2020;30:1436-1450.
13. Laubach HJ, Jakob PM, Loevblad KO, et al. A phantom for diffusion-weighted imaging of acute stroke. *J Magn Reson Imaging*. 1998;8:1349-1354.
14. Matsuya R, Kuroda M, Matsumoto Y, et al. A new phantom using polyethylene glycol as an apparent diffusion coefficient standard for MR imaging. *Int J Oncol*. 2009;35:893-900.
15. Gatidis S, Schmidt H, Martirosian P, Schwenzer NF. Development of an MRI phantom for diffusion-weighted imaging with independent adjustment of apparent diffusion coefficient values and T2 relaxation times. *Magn Reson Med*. 2014;72:459-463.
16. Lavdas I, Behan KC, Papadaki A, McRobbie DW, Aboagye EO. A phantom for diffusion-weighted MRI (DW-MRI). *J Magn Reson Imaging*. 2013;38:173-179.
17. Wang X, Reeder SB, Hernando D. An acetone-based phantom for quantitative diffusion MRI. *J Magn Reson Imaging*. 2017;46:1683-1692.
18. Fritz V, Martirosian P, Machann J, Daniels R, Schick F. A comparison of emulsifiers for the formation of oil-in-water emulsions: stability of the emulsions within 9 h after production and MR signal properties. *MAGMA*. 2022;35:401-410.
19. Machann J, Hasenbalg M, Dienes J, et al. Short-term variability of proton density fat fraction in pancreas and liver assessed by multiecho chemical-shift encoding-based MRI at 3T. *J Magn Reson Imaging*. 2022;56:1018-1026.
20. Israelachvili JN. *Intermolecular and Surface Forces*. Elsevier; 2011:676.
21. Tadros TF. Emulsion formation, stability, and rheology. In: Tadros TF, ed. *Emulsion Formation and Stability*. Wiley-VCH; 2013:1-75.
22. Kim BR, Song JS, Choi EJ, Hwang SB, Hwang HP. Diffusion-weighted imaging of upper abdominal organs acquired with multiple b-value combinations: value of normalization using spleen as the reference organ. *Korean J Radiol*. 2018;19:389-396.
23. Yoshikawa T, Kawamitsu H, Mitchell DG, et al. ADC measurement of abdominal organs and lesions using parallel imaging technique. *AJR Am J Roentgenol*. 2006;187:1521-1530.
24. Helenius J, Soinne L, Perkiö J, et al. Diffusion-weighted MR imaging in normal human brains in various age groups. *AJNR Am J Neuroradiol*. 2002;23:194-199.
25. Malyarenko DI, Swanson SD, Konar AS, et al. Multicenter repeatability study of a novel quantitative diffusion kurtosis imaging phantom. *Tomography*. 2019;5:36-43.
26. Portakal ZG, Shermer S, Jenkins C, et al. Design and characterization of tissue-mimicking gel phantoms for diffusion kurtosis imaging. *Med Phys*. 2018;45:2476-2485.
27. Mkam Tsengam IK, Omarova M, et al. Transformation of lipid vesicles into micelles by adding nonionic surfactants: elucidating the structural pathway and the intermediate structures. *J Phys Chem B*. 2022;126:2208-2216.
28. McHugh DJ, Zhou FL, Wimpenny I, et al. A biomimetic tumor tissue phantom for validating diffusion-weighted MRI measurements. *Magn Reson Med*. 2018;80:147-158.
29. Bojorquez JZ, Bricq S, Acquitter C, Brunotte F, Walker PM, Lalande A. What are normal relaxation times of tissues at 3 T? *Magn Reson Imaging*. 2017;35:69-80.
30. Tofts PS, Shuter B, Pope JM. Ni-DTPA doped agarose gel—a phantom material for Gd-DTPA enhancement measurements. *Magn Reson Imaging*. 1993;11:125-133.
31. Christoffersson JO, Olsson LE, Sjöberg S. Nickel-doped agarose gel phantoms in MR imaging. *Acta Radiol*. 1991;32:426-431.
32. Wagner F, Laun FB, Kuder TA, et al. Temperature and concentration calibration of aqueous polyvinylpyrrolidone (PVP) solutions for isotropic diffusion MRI phantoms. *PLoS One*. 2017;12:e0179276.

How to cite this article: Fritz V, Martirosian P, Machann J, Thorwarth D, Schick F. Soy lecithin: A beneficial substance for adjusting the ADC in aqueous solutions to the values of biological tissues. *Magn Reson Med*. 2022;1-10. doi: 10.1002/mrm.29543